

Kinematics of B–F Stars as a Function of Their Dereddened Color from Gaia and PCRV Data

G. A. Gontcharov*

Pulkovo Astronomical Observatory, Russian Academy of Sciences, Pulkovskoe
sh. 65, St. Petersburg, 196140 Russia

arXiv:1803.04055v1 [astro-ph.GA] 11 Mar 2018

*georgegontcharov@yahoo.com

Abstract

Parallaxes with an accuracy better than 10% and proper motions from the Gaia DR1 TGAS catalogue, radial velocities from the Pulkovo Compilation of Radial Velocities (PCRV), accurate Tycho-2 photometry, theoretical PARSEC, MIST, YAPSI, BaSTI isochrones, and the most accurate reddening and interstellar extinction estimates have been used to analyze the kinematics of 9543 thin-disk B–F stars as a function of their dereddened color. The stars under consideration are located on the Hertzsprung–Russell diagram relative to the isochrones with an accuracy of a few hundredths of a magnitude, i.e., at the level of uncertainty in the parallax, photometry, reddening, extinction, and the isochrones themselves. This has allowed us to choose the most plausible reddening and extinction estimates and to conclude that the reddening and extinction were significantly underestimated in some kinematic studies of other authors. Owing to the higher accuracy of TGAS parallaxes than that of Hipparcos ones, the median accuracy of the velocity components U , V , W in this study has improved to 1.7 km s^{-1} , although outside the range $-0.1^m < (B_T - V_T)_0 < 0.5^m$ the kinematic characteristics are noticeably biased due to the incompleteness of the sample. We have confirmed the variations in the mean velocity of stars relative to the Sun and the stellar velocity dispersion as a function of their dereddened color known from the Hipparcos data. Given the age estimates for the stars under consideration from the TRILEGAL model and the Geneva-Copenhagen survey, these variations may be considered as variations as a function of the stellar age. A comparison of our results with the results of other studies of the stellar kinematics near the Sun has shown that selection and reddening underestimation explain almost completely the discrepancies between the results. The dispersions and mean velocities from the results of reliable studies fit into a $\pm 2 \text{ km s}^{-1}$ corridor, while the ratios σ_V/σ_U and σ_W/σ_U fit into ± 0.05 . Based on all reliable studies in the range $-0.1^m < (B_T - V_T)_0 < 0.5^m$, i.e., for an age from 0.23 to 2.4 Gyr, we have found: $W = 7.15 \text{ km s}^{-1}$, $\sigma_U = 16.0e^{1.29(B_T - V_T)_0}$, $\sigma_V = 10.9e^{1.11(B_T - V_T)_0}$, $\sigma_W = 6.8e^{1.46(B_T - V_T)_0}$, the stellar velocity dispersions in km s^{-1} are proportional to the age in Gyr raised to the power $\beta_U = 0.33$, $\beta_V = 0.285$, and $\beta_W = 0.37$.

PACS numbers: 97.10.Zr; 98.10.+z; 98.35.Pr

Key words: Hertzsprung-Russell, color-magnitude, and color-color diagrams; Stellar dynamics and kinematics; Solar neighborhood in Galaxy.

INTRODUCTION

The dependence of kinematics on astrophysical characteristics of stars has been investigated for a long time (Parenago 1954, p. 139; Perryman 2009, pp. 302, 490). The dependence of the dispersions σ_U , σ_V , σ_W and means \overline{U} , \overline{V} , \overline{W} of the velocity components U , V , W in the rectangular Galactic coordinate system ¹ on the intercorrelating color, dereddened color, spectral type, effective temperature, and age for main-sequence (MS) B–F stars is particularly pronounced.

The quantities \overline{U} , \overline{V} , \overline{W} for a sample of stars with specific astrophysical characteristics taken with the opposite sign are considered as the components U_\odot , V_\odot , W_\odot of the solar motion relative to this sample, i.e., the peculiar solar motion toward the apex (Kulikovskii 1985, p. 74).

The quantities U , V , W are calculated from the Galactic longitude l , latitude b , distance R , or parallax ϖ as well as the proper motion components $\mu_l \cos(b)$ and μ_b and radial velocity V_r (Kulikovskii 1985, p. 74). Studies of the dependence of kinematic characteristics on astrophysical ones have reached a new level of accuracy and completeness after the appearance of the Hipparcos catalogue (ESA 1997) and its new version (van Leeuwen 2007) with highly accurate positions, parallaxes, and proper motions for tens of thousands of stars near the Sun, mostly within 200 pc.

Table 1 presents, in chronological order, the key studies of the dependence of these kinematic characteristics on the dereddened color or characteristics correlating with it for a large number of B–F stars near the Sun that have appeared after Hipparcos. These do not include the studies where kinematic characteristics are not matched with fairly accurate astrophysical ones. In addition, we do not consider the studies of separate small groups of stars or stars far from the Sun, because their kinematics can differ significantly from the overall kinematics of the local group of stars. In all of the studies under consideration the stellar positions, parallaxes, and proper motions were taken from Hipparcos. In the column ‘Sources of V_r ’ the cases of analyzing the kinematics without using any radial velocities are marked as ‘-’. A theory of such an analysis was given by Dehnen and Binney (1998), Mignard (2000), and Aumer and Binney (2009). Three popular catalogues of radial velocities of bright stars were used in the remaining studies: the Second Catalogue of Radial Velocities with Astrometric Data (CRVAD-2; Kharchenko et al. 2007), the Pulkovo Compilation of Radial Velocities (PCRV; Gontcharov 2006), and the Geneva-Copenhagen survey of the solar neighborhood (GCS; Nordström et al. 2004; Holmberg et al. 2007, 2009; Casagrande et al. 2011). The column ‘Argument’ gives the quantity on which the kinematic characteristics in the corresponding study depends ($(B_T - V_T)$ and $b - y$ were calculated from Tycho-2 (Høg et al. 2000) and Stroömgren photometry, respectively). The presence or absence of results for the corresponding characteristic in the study is marked in the columns ‘ σ_U ’, ‘ σ_V ’, ‘ σ_W ’ and ‘ $U_\odot V_\odot W_\odot$ ’.

The symbols representing the results of the studies under consideration in Figs. 1–5, where the kinematic characteristics are plotted against the dereddened color $(B_T - V_T)_0$ (the recalculation of the original arguments to $(B_T - V_T)_0$ is discussed below), are given in the column Designation. The results of the studies are indicated by separate signs for the subsamples into which the entire sample of stars was divided in the corresponding study. The results of Francis and Anderson (2009) are shown in Figs. 1a, 2a, 3, and 4 twice: before the exclusion of particular

¹ U and the X axis are directed toward the Galactic center, V and Y are in the direction of Galactic rotation, W and Z are directed toward the North Pole.

Table 1: Key studies of the dependence of kinematic characteristics on astrophysical ones for B–F stars near the Sun that have appeared after Hipparcos. $\Delta E(B_T - V_T)$ is the correction to the reddening adopted in the corresponding study. X denotes $(B_T - V_T)_0$.

Reference	Designation	Sources of V_r	Argument	σ_U	σ_V	σ_W	$U_\odot V_\odot W_\odot$	$\Delta E(B_T - V_T)$
Gómez et al. (1997)	Gray squares	Various	Age	+	+	+	–	0
Dehnen and Binney (1998)	Black triangles	–	$(B_T - V_T)$	+	–	–	+	$0.04 + 0.01X$
Mignard (2000)	Gray diamonds	–	Sp. type	+	+	+	+	0
Aumer and Binney (2009)	Black squares	–	$(B_T - V_T)_0$	+	+	+	–	$0.04 + 0.01X$
Francis and Anderson (2009)	Black diamonds	CRVAD-2	$(B_T - V_T)$	+	–	–	+	$0.08 - 0.05X$
Gontcharov (2012c)	Gray curve	PCRv	$(B_T - V_T)_0$	+	+	+	+	$0.24X^3 - 0.22X^2 + 0.07X$
Aghajani and Lindgren (2013)	Black circles	GCS	$(b - y)$	+	+	+	+	$-0.90X^3 + 1.63X^2 - 1.00X + 0.25$

stars from their sample (open black diamonds) and for the thin-disk stars (filled diamonds). The vertical bar near each sign indicates the formal error of the corresponding study. For all studies the errors of the dispersions and means of the velocities lie within the range $0.4\text{--}2 \text{ km s}^{-1}$ and, in some cases, they are smaller than the size of the sign in the figure. Figures 2 and 4 differ from Figs. 1 and 3, respectively, in that the corrections to the reddening adopted in the corresponding study that are discussed below were made in the results of the studies. They are given in the column ‘ $\Delta E(B_T - V_T)$ ’ of Table 1, where X denotes $(B_T - V_T)_0$. For σ_V/σ_U and σ_W/σ_U the influence of the corrections is small and, therefore, no analog without corrections is shown for Fig. 5. The thin stepwise curve in Figs. 1, 2, and 5 indicates the kinematic characteristics adopted in the Besançon model of the Galaxy (BMG) (Robin et al. 2003; Czekaj et al. 2014).

The results of this study based on TGAS and PCRv data are also shown in Figs. 1–5. For them, following Gómez et al. (1997) and Gontcharov (2012c), we applied a moving averaging. The stars were arranged by age $(B_T - V_T)_0$ and the sought-for kinematic characteristic was calculated for the subsample of stars with ordinal numbers from 1 to 500 (the bluest stars), then from 2 to 501, from 3 to 502, and so on. As a result, a set of similarly averaged values of $(B_T - V_T)_0$ was associated with the set of values of each kinematic characteristic. The results of Gontcharov (2012c) and this study are indicated by the gray and black curves, respectively (the gray band $\pm 2 \text{ km s}^{-1}$ in width is shown for clarity), while the results of Gómez et al. (1997) are indicated by the thin solid black line with gray squares strung on it to distinguish them from the remaining ones.

The discrepancies between the results of different studies visible in the figures often exceed considerably the declared formal errors. This study is devoted to explaining these discrepancies. It seems timely, because the original data for calculating the kinematic characteristics and the arguments on which they can depend have been updated significantly in recent years. In particular, Gontcharov (2017a) produced a new 3D reddening map, while Gontcharov and Mosenkov (2017a, 2017b) showed it to be one of the best maps within a few hundred pc of the Sun. In addition, the theoretical isochrones, for example, PARSEC (Bressan et al. 2012), MESA Isochrones and Stellar Tracks (MIST) (Paxton et al. 2011; Dotter 2016; Choi et al. 2016), Yale-Potsdam Stellar Isochrones (YaPSI) (Spada et al. 2017), and BaSTI (Pietrinferni et al. 2004), as well the population synthesis models (stellar population modeling) accompanying them have been improved compared to their previous analogs. They are already intensively used to test the dependences of kinematic characteristics on astrophysical ones (Czekaj et al. 2014).

However, the main data updates stem from the appearance of the first results of the Gaia space project (Gaia 2016) in September 2016. The Gaia DR1 Tycho-Gaia astrometric solution (TGAS) catalogue (Michalik et al. 2015) with accurate l , b , $\mu_l \cos(b)$, μ_b and ϖ for more than

two million stars from Tycho-2 is among them. In TGAS the parallaxes ϖ were determined by comparing the measured Gaia positions with the positions of the same stars from Hipparcos and Tycho-2.

In this study we calculated σ_U , σ_V , σ_W , U_\odot , V_\odot and W_\odot from the TGAS data and PCRV radial velocities and considered their dependences on $(B_T - V_T)_0$. The results obtained were compared with the mentioned results of other authors. The following factors can be responsible for the discrepancies found.

1. The first and new versions of Hipparcos were used in the studies before and after 2009, respectively, while TGAS was used in this study.
2. The radial velocities were taken from different sources or were not used at all.
3. Magnitude, distance, etc. constraints were imposed on the sample of stars, which led to various types of selection.
4. A particular astrophysical characteristic was used as an argument. The age calculation from the observed color by Gómez et al. (1997) introduces an additional uncertainty into their results.
5. Different reddening estimates were used when calculating the dereddened color from the observed one.

In this study we analyze all these factors and infer the role of each of them.

Note that the parameters of the linear Ogorodnikov-Milne model and the Oort constants A , B , C , and K related to them are not analyzed in this study, because they are calculated for stars near the Sun with a comparatively low accuracy. In this study, to take into account the Galactic rotation, we adopted $A = 15.3 \text{ km s}^{-1} \text{ kpc}^{-1}$ and $B = -11.9 \text{ km s}^{-1} \text{ kpc}^{-1}$ found by Bovy (2017) for comparatively distant TGAS stars.

ORIGINAL DATA

The distances R for TGAS stars estimated by Astraatmadja and Bailer-Jones (2016) based on ϖ and their errors $\sigma(\varpi)$ from TGAS are used in this study. These R slightly differ from the $R = 1/\varpi$ estimate primarily because the Lutz-Kelker and Malmquist biases (Perryman 2009, p. 208) were taken into account.

The TGAS authors recommended to add an uncertainty of 0.3 mas, which describes the disregarded systematic errors in ϖ (Gaia 2016), to their formal parallax error $\sigma(\varpi)$. However, having investigated their samples of clump giants from TGAS, Gontcharov (2017b) and Gontcharov and Mosenkov (2017a) showed that the systematic errors of the TGAS parallaxes do not exceed 0.2 mas within 700 pc of the Sun. This value was added to $\sigma(\varpi)$ in this study.

Following the recommendation of Dehnen and Binney (1998), for this study we selected stars with $\sigma(\varpi)/\varpi < 0.1$. This corresponds to $R < 330 \text{ pc}$. 67% and 95% of the stars in the final sample are within 135 and 225 pc of the Sun, respectively. The median distance from the Sun for the sample stars changes approximately linearly with $(B_T - V_T)_0$ from 170 pc at

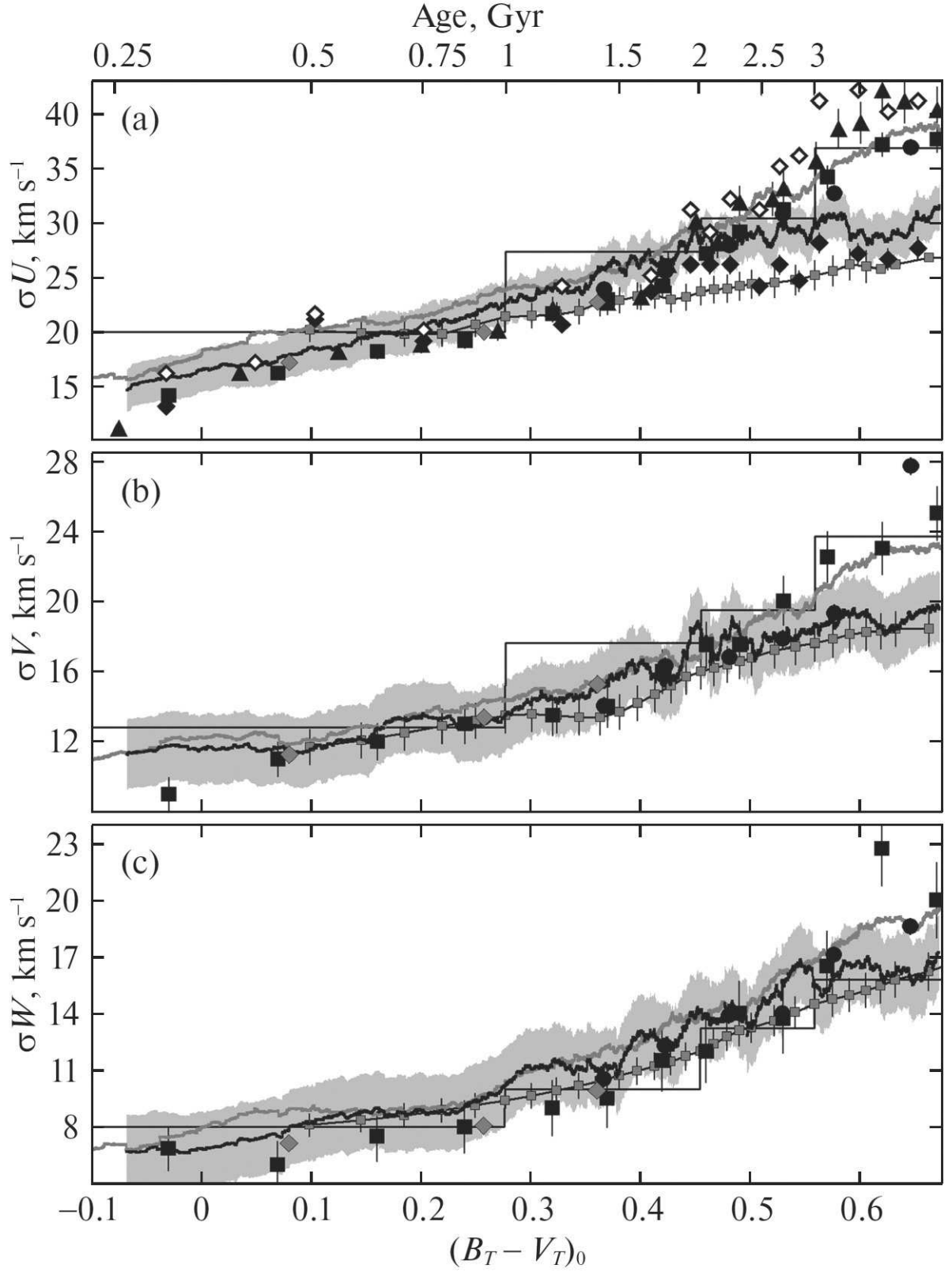


Figure 1: Dispersions (a) σ_U , (b) σ_V , and (c) σ_W versus $(B_T - V_T)_0$ and age for the studies specified in Table 1 before applying the reddening corrections. The black curve represents our result; the stepwise polygonal curve represents the BMG. The gray band $\pm 2 \text{ km s}^{-1}$ in width is shown for clarity.

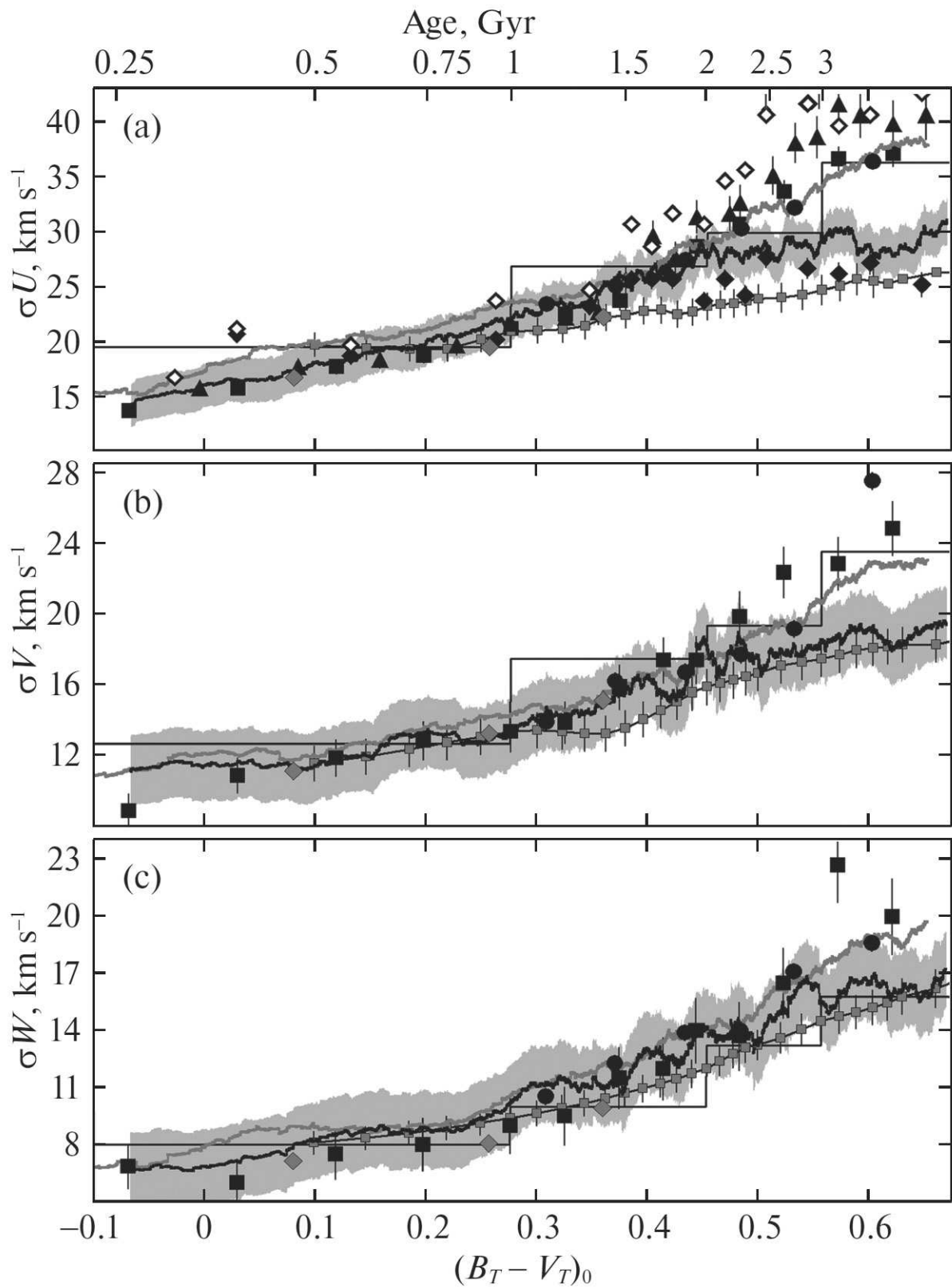


Figure 2: Same as Fig. 1 after applying the reddening corrections.

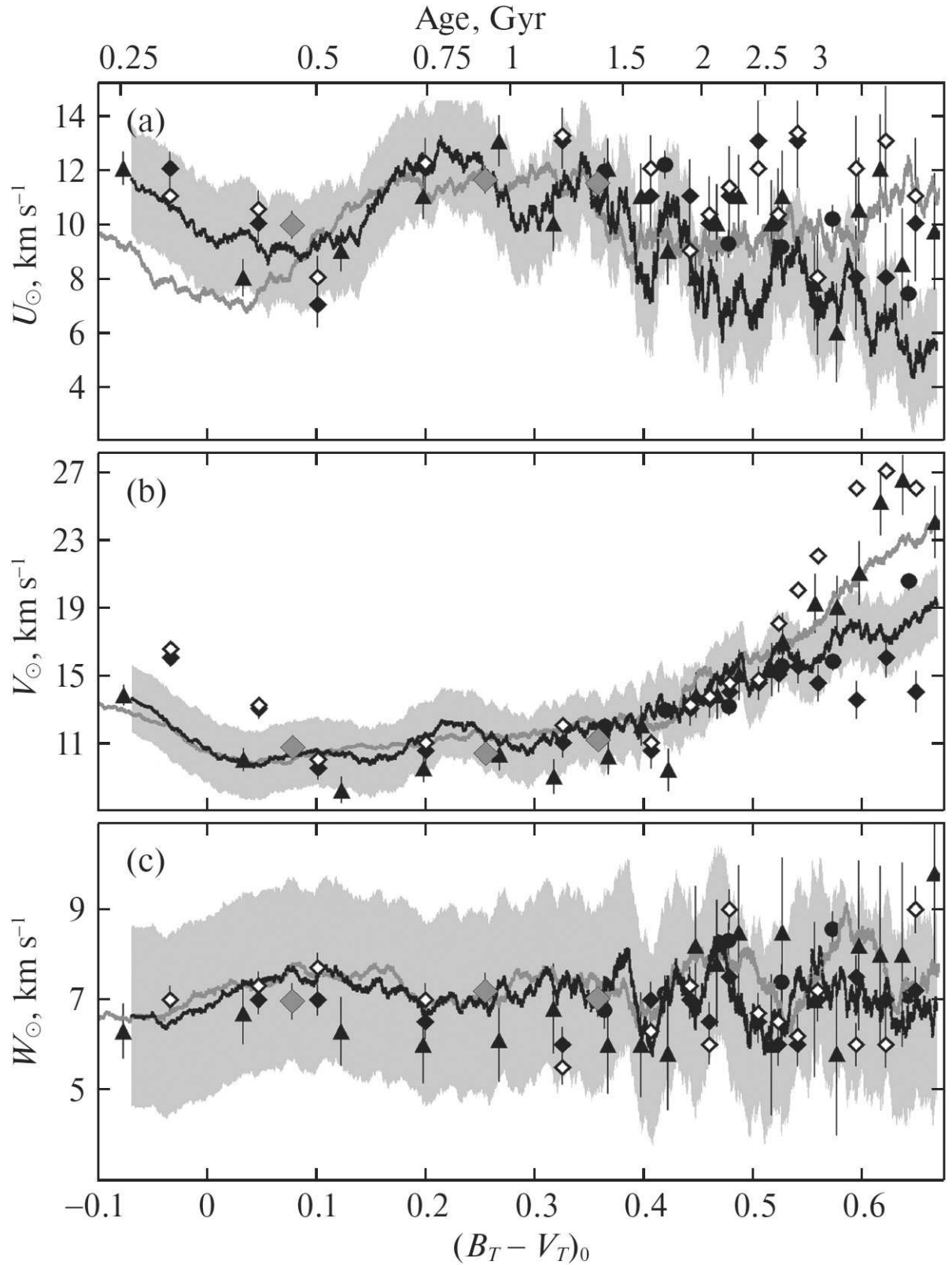


Figure 3: Solar velocity components (a) U_{\odot} , (b) V_{\odot} , and (c) W_{\odot} versus $(B_T - V_T)_0$ and age for the studies specified in Table 1 before applying the reddening corrections. The black curve represents our result. The gray band $\pm 2 \text{ km s}^{-1}$ in width is shown for clarity.

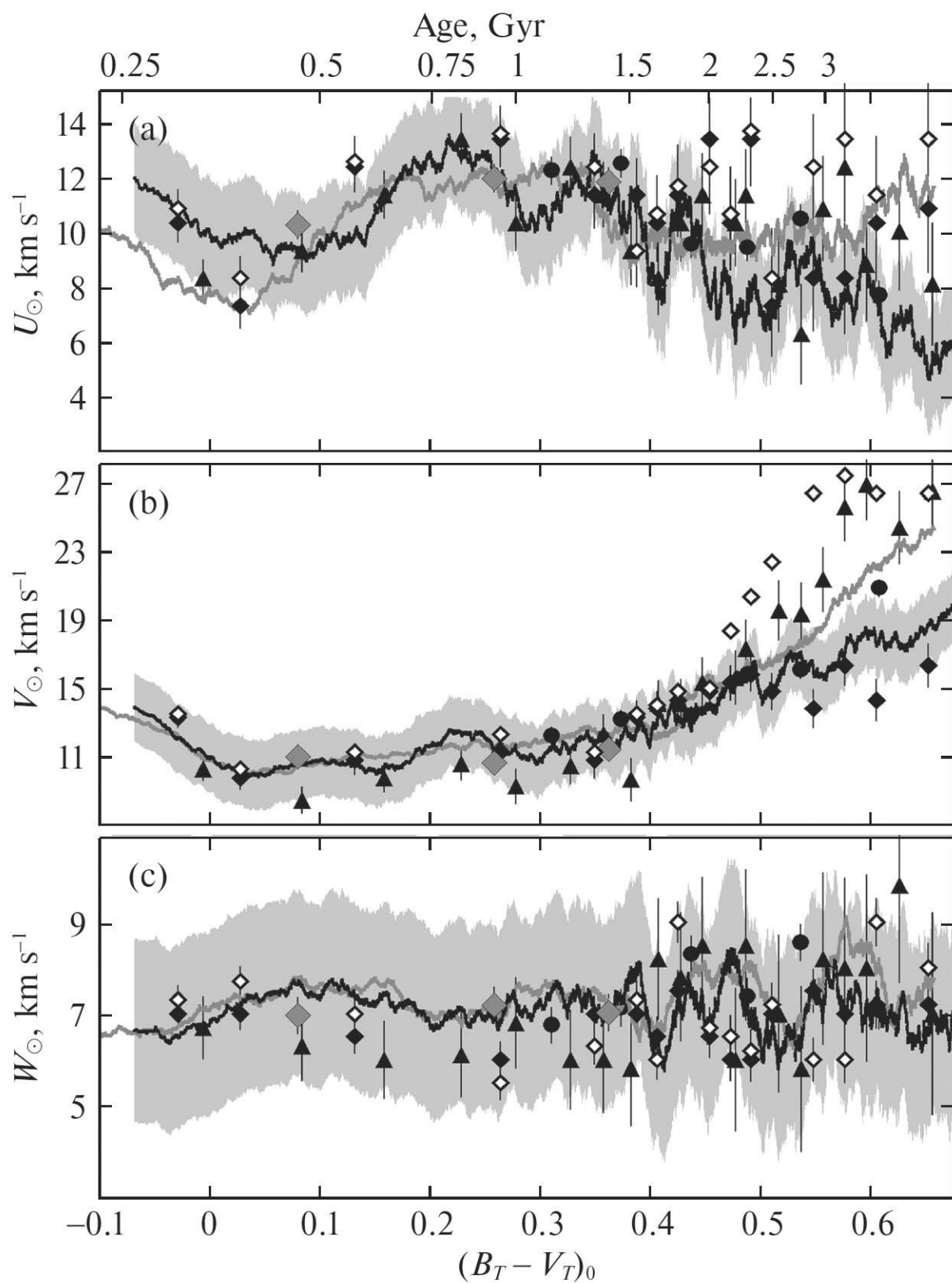


Figure 4: Same as Fig. 3 after applying the reddening corrections.

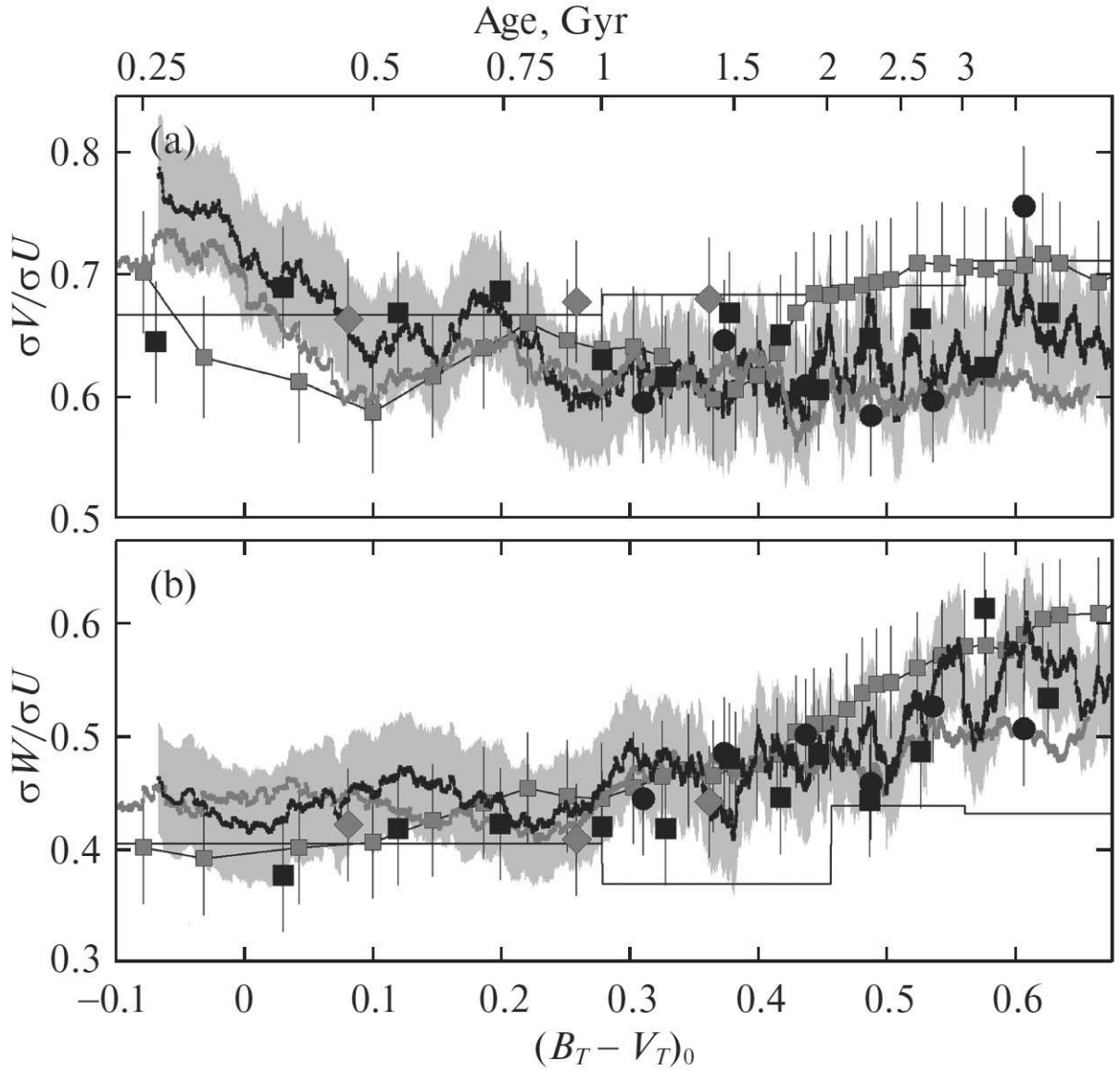


Figure 5: Ratios (a) σ_V/σ_U and (b) σ_W/σ_U versus $(B_T - V_T)_0$ and age for the studies specified in Table 1 after applying the reddening corrections. The black curve represents our result; the stepwise polygonal curve represents the BMG. The gray band ± 0.05 in width is shown for clarity.

$(B_T - V_T)_0 = -0.1^m$ to 60 pc at $(B_T - V_T)_0 = 0.7^m$. The median value is $\sigma(\varpi)/\varpi = 0.045$. Since the sample stars are close to the Sun, this gives a relative error in R of 4.5% .

The errors in $\mu_l \cos(b)$ and μ_b for all of the selected stars are less than 0.3 mas yr $^{-1}$. This is smaller than the analogous errors in Hipparcos approximately by a factor of 3. Such an increase in accuracy actually excludes the proper motions from the sources of errors in U , V , W , and they are now determined by the errors in R and V_r . Indeed, for the overwhelming majority of stars 0.3 mas yr $^{-1}$ corresponds to a relative error much smaller than 4.5% . Therefore, the error in the tangential velocity components $V_l = 4.74R\mu_l \cos(b)$ and $V_b = 4.74R\mu_b$ is determined by the error in R and is less than 5% . This corresponds to $\sigma(V_l) < 1.25$, $\sigma(V_b) < 1.25$ km s $^{-1}$, given that V_l and V_b do not exceed 25 km s $^{-1}$ in absolute value for the overwhelming majority of stars. The median error in V_l and V_b is 1 km s $^{-1}$.

The radial velocities for the TGAS stars under consideration are presented in the Radial Velocity Experiment (RAVE) (Kunder et al. 2017) and LAMOST Spectroscopic Survey of Galactic Anti-Center (Tian et al. 2015) projects, the mentioned CRVAD-2, PCRV, and GCS catalogues, and many small catalogues. GCS was used in the PCRV after allowance made for the systematic errors, including the error in V_r as a function of $(B - V)$ reaching $\Delta V_r = 1$ km s $^{-1}$ at $(B - V) = 0.2^m$, which is especially important for our study. The CRVAD-2 authors ignored these errors and simply averaged the PCRV and GCS data for the corresponding stars. Thus, they actually transferred the GCS errors reduced by half to CRVAD-2. The GCS, RAVE, and LAMOST catalogues refer mainly only to MS F–G stars. In addition, RAVE and LAMOST cover only part of the sky and exhibit systematic errors in V_r reaching $\Delta V_r = 1.5$ km s $^{-1}$ for RAVE (Gontcharov 2007) and $\Delta V_r = 5.7$ km s $^{-1}$ for LAMOST (Tian et al. 2015). Tian et al. (2015) showed that such errors could distort severely the kinematic characteristics. Thus, the PCRV is the only catalogue of V_r in which the systematic errors in V_r were determined and taken into account. Therefore, this study is restricted to using the PCRV. Other catalogues of V_r are planned to be used after investigating their systematic errors.

The PCRV contains the radial velocities for 35493 stars from the Hipparcos catalogue. The median error in V_r for the TGAS stars under consideration is 0.8 km s $^{-1}$, with V_r being more accurate than 2 km s $^{-1}$ for the overwhelming majority of stars and more accurate than 5 km s $^{-1}$ for all stars.

Thus, the errors in U , V , and W for the stars under consideration are determined by the errors in R and V_r . From the formulas provided by Kulikovskii (1985, p. 74), given the errors in V_l , V_b , and V_r of 1.25 , 1.25 , and 2 km s $^{-1}$, respectively, for the overwhelming majority of stars under consideration (the median ones are 1 , 1 , and 0.8 km s $^{-1}$), we find that the errors in U , V , and W for them do not exceed 2.5 km s $^{-1}$ (the median error is 1.7 km s $^{-1}$). At present, this is a record high accuracy of the data used to calculate the kinematic characteristics. Note that this progress was achieved mainly through the high accuracy of TGAS parallaxes.

However, the kinematic characteristics obtained in this study are the result of averaging 500 original values. Therefore, the formal error of such a mean must be much smaller than the error in the velocity of an individual star and smaller than the thickness of the black curve in the figures. Formally, the accuracy of the results of this study is considerably higher than the typical accuracy of 0.4 – 2 km s $^{-1}$ in the remaining studies under consideration, because ϖ and μ from Hipparcos were replaced by their more accurate values from TGAS. However, this study, along with all the remaining ones, may disregard some systematic errors. The above accuracy was then overestimated. We note unresolved binary stars (Gontcharov et al. 2001) as an obvious

source of such systematic errors. Therefore, for clarity, the gray band along the black curve in all figures indicates not the error of the mean for 500 stars but an upper limit for the accuracy of the studies under consideration.

Most of the studies mentioned in Table 1 used $(B_T - V_T)$ or $(B_T - V_T)_0$ as an argument. Therefore, $(B_T - V_T)_0$ was used as an argument for this study as well. The Tycho-2 photometry is accurate ($\sigma(B_T) < 0.05^m$, $\sigma(V_T) < 0.05^m$, the median accuracy is higher than 0.02^m) under the constraints $B_T < 11^m$ and $V_T < 10.7^m$. They were applied in this study. In addition, the constraint $(B_T - V_T)_0 < 0.7^m$ was imposed on the sample to exclude the giants and MS stars of late types. As a result, 9567 stars remained in the sample. Note that due to the small fraction of stars with measured V_r , this sample, like any sample from Table 1, is not complete in the space under consideration. Under the same selection conditions, but without restricting ourselves to the PCRV stars, we would select 30509 and 97253 stars from Hipparcos and TGAS, respectively.

To exclude the stars that do not correspond to the thin-disk kinematics, for example, high-velocity OB stars (Gontcharov and Bajkova 2013) and hot subdwarfs (Gontcharov et al. 2011), we applied the criterion from Aumer and Binney (2009). A star was excluded if its total space velocity $(U^2 + V^2 + W^2)^{1/2}$ was larger than $3.5(\sigma_U^2 + \sigma_V^2 + \sigma_W^2)^{1/2}$ calculated, as described previously, as a moving average for the corresponding window of 500 stars. Since the exclusion of stars reduces the velocity ellipsoid, the process is repeated in iterations. We needed three instead of six iterations in Aumer and Binney (2009). We rejected 24 stars instead of 55 in Aumer and Binney (2009); 9543 thin-disk stars remained in the final sample.

The reddening $E(B_T - V_T) = (B_T - V_T) - (B_T - V_T)_0$ and interstellar extinction A_{V_T} were taken into account in this study in accordance with the 3D reddening $E(J - K_s)$ map constructed by Gontcharov (2017a) from 2MASS photometry (Skrutskie et al. 2006). Under the assumption of $E(B - V) = 1.655E(J - K_s)$ this map gives a 3D $E(B - V)$ map and, together with the extinction-to-reddening $R_V = A_V/E(B - V)$ map from Gontcharov (2012a), a 3D A_V map. Let us justify the use of precisely these reddening and extinction estimates.

REDDENING

Since the visible range and extinction laws close to the law from Cardelli et al. (1989) with $A_V = 3.1E(B - V)$ are considered in all of the above studies, the extinction estimate is uniquely related to the reddening estimate. Below in this study we use everywhere the extinction law with $A_{B_T} = 1.36A_V$, $A_{V_T} = 1.06A_V$, $A_b = 1.24A_V$ and $A_y = A_V$ adopted in the PARSEC database and very close to the extinction law from Cardelli et al. (1989).

Let us compare the reddening estimates adopted in the studies from Table 1. Gómez et al. (1997) calculated the age from the positions of stars on the Hertzsprung–Russell (HR) diagram relative to the isochrones by first estimating the effective temperature and metallicity from Strömgren photometry or spectroscopic data and the reddening from Strömgren photometry. Apparently, their reddening estimates may be deemed sufficiently accurate. Mignard (2000) did not need to take into account the reddening, because the spectral classification of stars was used as an argument. Aumer and Binney (2009) adopted zero reddening within 70 pc of the Sun and a subsequent growth in reddening $E(B - V)$ with distance by 0.47^m kpc^{-1} . They noted that their revision of the reddening estimates compared to the preceding studies changed significantly the estimates of some kinematic characteristics. Gontcharov (2012c) estimated the reddening

from the extinction ratio based on the 3D model from Gontcharov (2009b, 2012b) and the extinction-to-reddening ratio $R_V = A_V/E(B-V)$ based on the 3D map of spatial R_V variations from Gontcharov (2012a). The new 3D reddening map from Gontcharov (2017a) shows that Gontcharov (2012c) overestimated the reddening of blue stars. Aghajani and Lindegren (2013) adopted the reddening from GCS calculated from Strömgren photometry. In the remaining studies the authors did not specify how the reddening was taken into account. However, the star selection methods specified by the authors allowed me to reconstruct (1) the composition of the samples for all of the mentioned studies, except for Gómez et al. (1997), (2) the distribution of the samples in $(B_T - V_T)_0$ and $(B_T - V_T)$, and (3) the mean reddening estimates adopted by the authors for each subsample. For the subsamples of Mignard (2000) we calculated new means $\overline{(B_T - V_T)_0}$ slightly differing from the original ones: $\overline{(B_T - V_T)_0} = 0.08^m$, 0.267^m , and 0.375^m for A0–A5, A5–F0, and F0–F5 stars, respectively. The calibration $(B_T - V_T)_0 = 16(b - y)^3 - 7(b - y)^2 + 2.42(b - y) - 0.08$ in accordance with the PARSEC database was adopted for the results of Aghajani and Lindegren (2013). As a result, it was established that Dehnen and Binney (1998) adopted reddening estimates close to those from Aumer and Binney (2009), i.e., close to 0 for most stars, while Francis and Anderson (2009), apparently, did not take into account the reddening at all.

The positions of the 9543 stars under consideration on the HR $(B_T - V_T)_0 - M_{V_T}$ diagram are shown in Fig. 6, where $(B_T - V_T)_0$ was not corrected for reddening, while M_{V_T} was not corrected for extinction A_{V_T} (Fig. 6a) or was corrected in accordance with the estimates of Aumer and Binney (2009) (Fig. 6b), GCS (Fig. 6c) used by Aghajani and Lindegren (2013), Arenou et al. (1992) (Fig. 6d), and Gontcharov (2012a, 2017a) (Fig. 6e). We chose precisely these reddening estimates, because many other popular estimates cannot be used in the solar neighborhood $R < 330$ pc under consideration, as was pointed out by their authors. The estimates by Schlegel et al. (1998), Meisner and Finkbeiner (2015), Green et al. (2015), and others are inapplicable here (Gontcharov 2017a; Gontcharov and Mosenkov 2017b).

The lines in Fig. 6 indicate three sets of PARSEC and MIST isochrones for 0.1, 1, and 3 Gyr (from left to right) and the following metallicities: $\mathbf{Z} = 0.0152$, $\mathbf{Y} = 0.2756$ (solar metallicity according to Bressan et al. (2012)) for PARSEC 0.1 and 1 Gyr and $\mathbf{Z} = 0.0142$, $\mathbf{Y} = 0.2738$ for 3 Gyr; MIST initial $\mathbf{Y} = 0.27$, initial $\mathbf{Z} = 0.0142$, actual $\mathbf{Z} = 0.0156$. In contrast to other models, MIST estimates the increase in metallicity as the star evolves and can take into account the stellar rotation. When choosing the isochrones, we took into account the mean metallicity–age relation for thin-disk stars (Haywood 2006). The isochrones for 0.1 Gyr may be deemed as the zero-age MS.

A sharp decrease in the number of stars at $(B_T - V_T)_0 > 0.5^m$ rightward of the 3-Gyr isochrones can be seen in Fig. 6. This is how the magnitude limitation of the Hipparcos catalogue and, subsequently, the PCRV manifested itself: these catalogues are much more complete with regard to B–A than F–G dwarfs (this can be seen, for example, in Fig. 6 from the PCRV description by Gontcharov (2006)). Consequently, the kinematic characteristics for the range $0.5^m < (B_T - V_T)_0 < 0.7^m$ must be distorted by selection more severely than those for the range $(B_T - V_T)_0 < 0.5^m$.

We see that for 0.1 Gyr the PARSEC and MIST isochrones almost coincide at $M_{V_T} > 3^m$; otherwise they diverge by no more than $\Delta(B_T - V_T)_0 = 0.05^m$. Much of this divergence is caused by allowance for the stellar rotation in MIST.

YaPSI and BaSTI give no isochrones for B_T and V_T , but all four isochrones for 0.1 Gyr

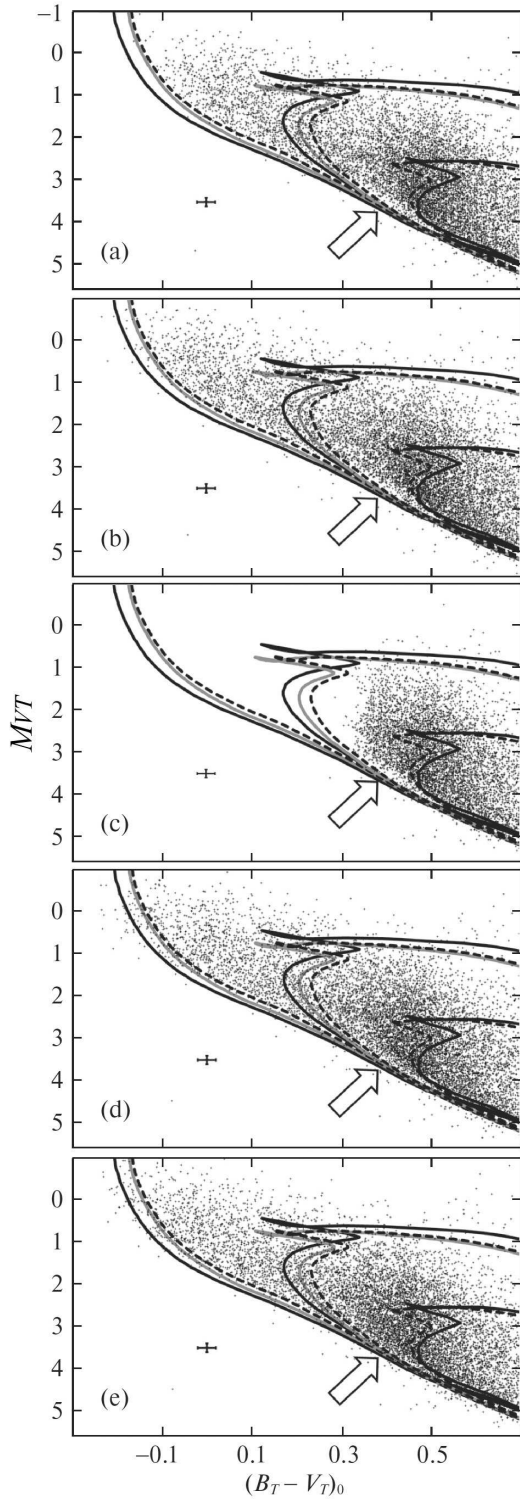


Figure 6: The stars under consideration on the HR $(B_T - V_T)_0 - M_{V_T}$ diagram uncorrected for reddening and extinction (a) and corrected in accordance with the estimates of Aumer and Binney (2009) (b), GCS (c), Arenou et al. (1992) (d), and Gontcharov (2012a, 2017a) (e). The lines indicate three sets of PARSEC (black solid curves) and MIST (with (black dashed curves) and without (gray solid curves) allowance for the stellar rotation) isochrones for 0.1, 1, and 3 Gyr (from left to right) and the metallicities specified in the text. The cross indicates the median errors of the data due to the photometric and parallax errors.

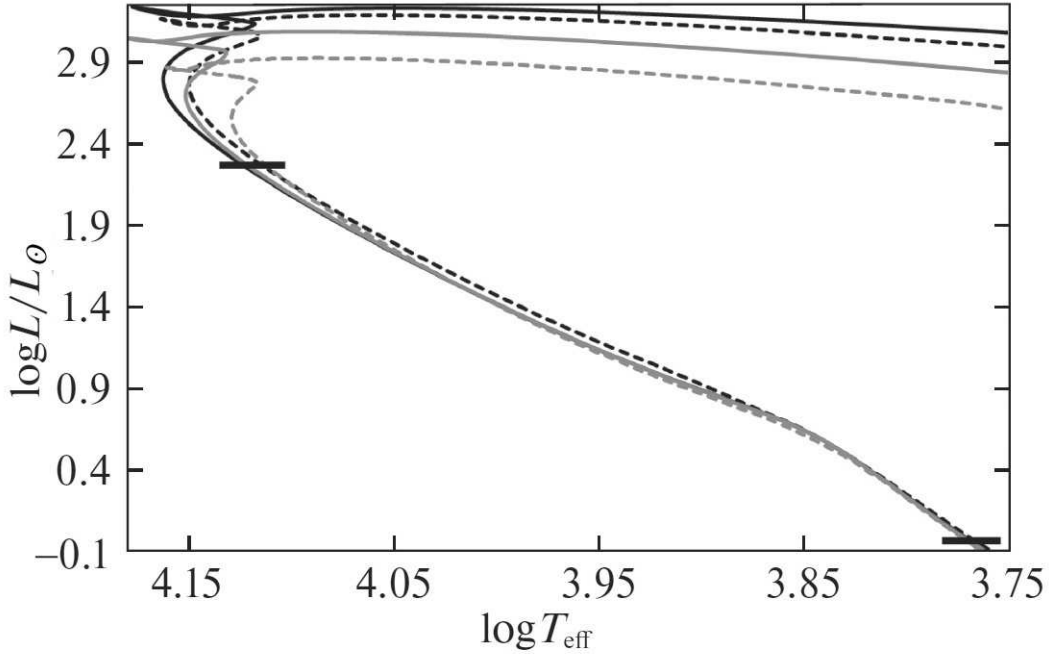


Figure 7: PARSEC (black solid curve), MIST (black dashed curve), YaPSI (gray solid curve), and BaSTI (gray dashed curve) isochrones on the HR effective temperature–luminosity diagram for an age of 0.1 Gyr and the metallicities specified in the text. The thick horizontal lines mark the luminosity range of interest to us.

can be compared on the effective temperature–luminosity diagram shown in Fig. 7. Here, $\mathbf{Z} = 0.0162$, $\mathbf{Y} = 0.28$ for YaPSI and $\mathbf{Z} = 0.014$, $\mathbf{Y} = 0.263$ for BaSTI. The thick horizontal lines mark the luminosity range $-0.04 < \log(L/L_{\odot}) < 2.27$ corresponding to the range $0^m < M_{V_T} < 5^m$ of interest to us. We see that here the YaPSI isochrone almost coincides with PARSEC, while BaSTI is located approximately between PARSEC and MIST. The discrepancy between the 0.1 Gyr isochrones is comparable to the errors of the photometry used and the error in the $E(B_T - V_T)$ estimates (for example, 0.03^m for Arenou et al. (1992) and 0.04^m for Gontcharov (2017a)). Therefore, the positions of the stars relative to the isochrones can be used to choose the best source of reddening estimates.

The arrow in Fig. 6 indicates the region of the HR diagram that is apparently most sensitive to the reddening and extinction estimates: the isochrones here almost coincide, while the number of stars is great. In this region on panel (a) the cloud of stars is offset from the isochrones, forming an unreasonable gap. It is retained on panels (b) and (c), shrinks noticeably on panel (d), and disappears on panel (e). This means that the mean reddening of the stars in this region of the diagram differs noticeably from zero, it was significantly underestimated by Aumer and Binney (2009) and Aghajani and Lindegren (2013), was slightly underestimated by Arenou et al. (1992), and was estimated most accurately by Gontcharov (2017a). The same conclusion can be drawn from the upper left part of the graphs, where the variant with zero reddening, and Aumer and Binney (2009) demonstrate a clearly insufficient number of youngest stars. The mean reddening $E(B_T - V_T)$ for the stars under consideration is 0.063^m , 0.045^m , and 0.024^m , as inferred by Gontcharov (2017a), Arenou et al. (1992), and Aumer and Binney (2009), respectively.

Adopting the reddening estimates from Gontcharov (2017a) as the most accurate ones, we

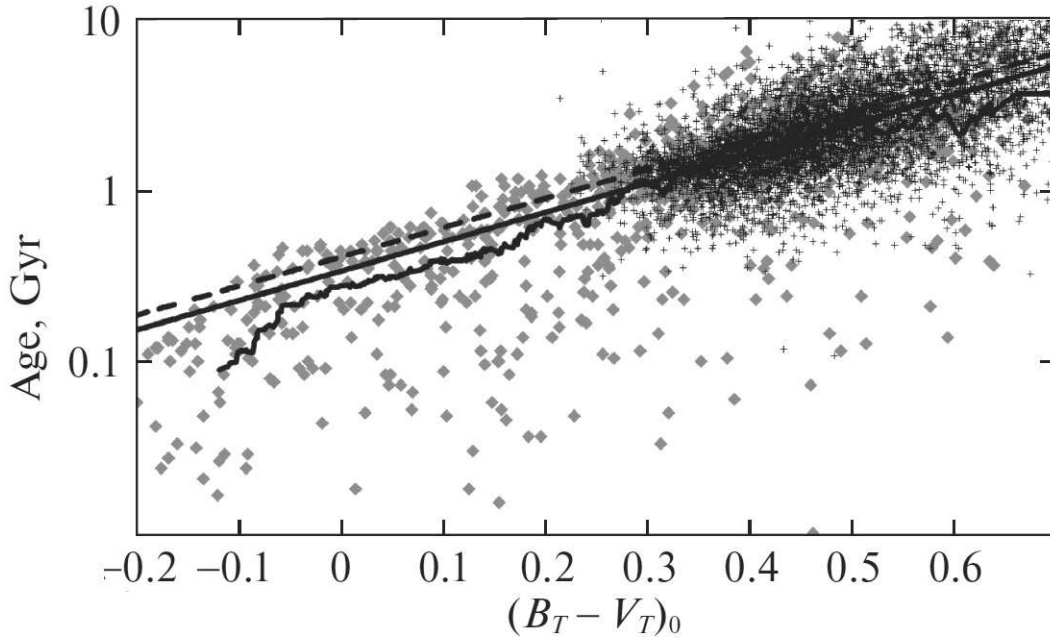


Figure 8: Age in Gyr versus $(B_T - V_T)_0$ for the GCS stars (black dots, the fit by the black solid line) and 1000 TRILEGAL simulated stars with the properties of the stars of this study (gray diamonds, the black polygonal curve is the moving average over 33 points). The black dashed curve is the fit of the previous GCS versions.

will add the corrections of the remaining studies for $E(B_T - V_T)$ from the column ‘ $\Delta E(B_T - V_T)$ ’ of Table 1 to $(B_T - V_T)_0$. The results of all studies corrected in this way are shown in Figs. 2, 4, and 5 (only the abscissas, but not the ordinates change). When comparing Figs. 2 and 4 with Figs. 1 and 3, we see that the results come significantly closer together.

AGE

A correlation between the dereddened color and age for MS B-F stars was pointed out by the authors of all studies from Table 1. The age estimates obtained by Casagrande et al. (2011) in the latest GCS version from an analysis of the positions of GCS stars relative to the PARSEC and BaSTI isochrones on the HR diagram are among the most accurate ones. Preliminary estimates of the metallicity of each star were used for this purpose. Several age estimates were obtained for each star, depending on the set of isochrones used and the method of calculation: the median, most probable, etc. However, they agree well in the range $(B_T - V_T)_0 < 0.7^m$ we consider. Below we use the median age estimate from the BaSTI isochrones. Figure 8 shows the relation between the age in Gyr and $(B_T - V_T)_0$ for the GCS stars. In this case, $(B_T - V_T)_0$ was calculated from the reddening from the map of Gontcharov (2017a). The black solid line indicates the following relation calculated for the GCS stars by the least-squares method:

$$T = 0.34e^{3.9(B_T - V_T)_0} \quad (1)$$

The relation $T = 0.41e^{3.9(B_T - V_T)_0}$ derived by Gontcharov (2012) from the previous GCS versions (Nordström et al. 2004; Holmberg et al. 2007, 2009) is indicated in Fig. 8 by the dashed line. The change of the coefficient in the relation is caused by the change of the calibrations

in the latest GCS version. Although GCS contains no blue stars, as can be seen from Fig. 8, extrapolating these relation to the range $(B_T - V_T)_0 < 0.25^m$ gives quite plausible age estimates.

Figure 8 also shows the result of simulating the sample of TGAS stars considered in this study using the TRIdimensional model of thE GALaxy (TRILEGAL; Girardi et al. 2005): 1000 simulated stars are indicated by the gray diamonds. TRILEGAL also accurately reproduces the distribution of stars on the HR diagram. The constraints $\sigma(\varpi)/\varpi < 0.1$ and $V_T < 10.7^m$ are seen to have deprived the sample of many blue ($(B_T - V_T)_0 < -0.1^m$) and red ($(B_T - V_T)_0 > 0.5^m$) stars.

For the TRILEGAL stars the dependence of the age on $(B_T - V_T)_0$ is indicated in Fig. 8 by the black polygonal curve, the result of moving averaging over 33 points. There is good agreement between the dependences for GCS and TRILEGAL, although the downward deflection of the polygonal curve at $(B_T - V_T)_0 < -0.1^m$ and $(B_T - V_T)_0 > 0.5^m$ confirms that in these ranges the sample under consideration is significantly incomplete with regard to the oldest stars and, hence, stars with a larger velocity dispersion. Consequently, the sample under consideration is comparable in completeness and accuracy of kinematic characteristics to other studies from Table 1 only in the range $-0.1^m < (B_T - V_T)_0 < 0.5^m$.

As a result, relation (1) was adopted everywhere in this study. In particular, it was used to calculate $(B_T - V_T)_0$ from the age for the results of Gómez et al. (1997). Relation (1) gives the age of an individual star with a very low accuracy of 50–100% and can be used only for the age statistics of a large number of stars.

The uniqueness of relation (1) allows us to plot the age scale on all figures in addition to the $(B_T - V_T)_0$ scale and to estimate the age dependences of the dispersions σ_U , σ_V and σ_W for the range of ages from 0.23 to 2.4 Gyr, which corresponds to $-0.1^m < (B_T - V_T)_0 < 0.5^m$. The generally known proportionality

$$\sigma \sim T^\beta. \quad (2)$$

is confirmed in this study. An overview of previous β determinations was given, for example, by Aumer and Binney (2009) and Sharma et al. (2014): $0.27 < \beta_{U,V} < 0.39$ and $0.33 < \beta_W < 0.54$ are typical for the thin disk.

The exponents β found are compared with the results of other studies in Table 2. For the studies from Table 1 two numbers separated by a slash are specified here: the original β and β for the range $-0.1^m < (B_T - V_T)_0 < 0.5^m$ after applying the reddening corrections. The second value is more suitable for a comparison with the results of this study. The exponents β from the results of the first (Nordström et al. 2004) and third (Holmberg et al. 2009) GCS versions are given only for comparison, because they were actually replaced by the new values obtained by Aghajani and Lindegren (2013) from the same data. Note that the previously specified systematic errors in V_r from GCS did not manifest themselves in these results.

It can be seen from Table 2 that β obtained in this study are close to the results of Gontcharov (2012c), noticeably larger than β from Gómez et al. (1997), and slightly smaller than the remaining ones. Narrowing the range of colors/ages and applying the reddening corrections reduced noticeably many of β , eliminated the extreme values, and placed the results of Aumer and Binney (2009), Gontcharov (2012c), Aghajani and Lindegren (2013), and this study in the narrow ranges $0.29 < \beta_U < 0.37$, $0.24 < \beta_V < 0.33$ and $0.32 < \beta_W < 0.40$ (the agreement of the results in Fig. 2 implies the agreement of β). Consequently, an accurate allowance for reddening and the systematic errors of the original data is needed for the conclusions about the kinematic characteristics to be reached.

Table 2: Exponents β in the dependence (2).

Reference	β_U	β_V	β_W
Gómez et al. (1997)	0.15 / 0.15	0.24 / 0.22	0.35 / 0.32
Nordström et al. (2004)	0.31	0.34	0.47
Holmberg et al. (2009)	0.39	0.40	0.53
Aumer and Binney (2009)	0.31 / 0.35	0.43 / 0.33	0.45 / 0.38
Gontcharov (2012c)	0.31 / 0.29	0.24 / 0.24	0.35 / 0.32
Aghajani and Lindegren (2013)	0.38 / 0.37	0.51 / 0.32	0.47 / 0.40
This study	0.31	0.25	0.38

OTHER SOURCES OF DISCREPANCIES

In Table 2 for the results of Gómez et al. (1997) β are very small. The corresponding deviation of the results of Gómez et al. (1997) from the remaining ones can also be seen in Figs. 1 and 2: the gray squares are shifted from the remaining results upward at $(B_T - V_T)_0 < 0.15^m$ and downward at $(B_T - V_T)_0 > 0.3^m$. The results of Francis and Anderson (2009) for the thin-disk stars, i.e., the filled diamonds (in contrast to the open ones) for σ_U in Figs. 1a and 2a, look the same.

This is the result of an excessively stringent and color- or age-independent constraint in the selection of thin-disk stars: Gómez et al. (1997) rejected the stars with a space velocity $(U^2 + V^2 + W^2)^{1/2} > 65 \text{ km s}^{-1}$; Francis and Anderson (2009) rejected 5660 stars (28% of their sample) with $(U^2 + V^2 + W^2)^{1/2} > 84 \text{ km s}^{-1}$. As a result, an admixture of stars that do not belong to the thin disk must be retained among the blue stars, while among the red stars, on the contrary, the fastest thin-disk stars were removed.

Our test showed that if the same constraints were imposed on the sample of Gontcharov (2012c), then more than 10% of the stars would be excluded from it. In this case, the dependences marked by the gray curves in Figs. 1 and 2 are shifted downward and turn out to be close to the filled black diamonds (the results of Francis and Anderson (2009)) and the gray squares (the results of Gómez et al. (1997)). The results of Francis and Anderson (2009), i.e., the positions of the filled diamonds relative to the open ones in Figs. 3b and 4b, show that such an exclusion of the fastest stars also affects the dependence of V_\odot on $(B_T - V_T)_0$, but only in the range $(B_T - V_T)_0 > 0.5^m$.

Thus, the deviation of the results of Gómez et al. (1997) and Francis and Anderson (2009) for the thin-disk stars from the results of other authors is explained by an incorrect selection criterion producing strong selection. However, the thin-disk stars should be isolated. Otherwise, the admixtures distort the results as much as, for example, the open diamonds in Figs. 1a, 2a, 3, and 4 deviate upward from the remaining results. Apparently, in Figs. 2a and 4b at $(B_T - V_T)_0 > 0.4^m$ the results of Francis and Anderson (2009) before and after the rejection of stars (open and filled diamonds) show the upper and lower limits between which all plausible results must be located.

However, the deviation of the results of Francis and Anderson (2009) from the remaining ones at $(B_T - V_T)_0 = 0.45^m$ and 0.49^m in Fig. 4a requires a different explanation. The previously mentioned systematic errors in V_r from CRVAD-2 used by them can be the culprit here.

Another discrepancy can be seen in Figs. 1–4: at $-0.05^m < (B_T - V_T)_0 < 0.1^m$ and $0.5^m < (B_T - V_T)_0 < 0.7^m$ the results of this study deviate noticeably from the results of a similar study by Gontcharov (2012c). Both were obtained using V_r from the PCRV. This forces us to suggest either selection, not due to the PCRV, or a systematic difference between the TGAS and Hipparcos parallaxes and proper motions as a cause of the discrepancies. Indeed, in the range $0.5^m < (B_T - V_T)_0 < 0.7^m$ the sample of Gontcharov (2012c) contains more than 1500 stars that are absent in TGAS, although they are present in Hipparcos. The causes of their absence in TGAS are comparatively close dwarfs (mostly closer than 70 pc) with very large proper motions, many of which are binary and variable stars. After their test exclusion from the sample of Gontcharov (2012c), the dependences of the kinematic characteristics on $(B_T - V_T)_0$ in the range $0.5^m < (B_T - V_T)_0 < 0.7^m$ coincided, within the error limits, with the results of this study. Thus, it is confirmed once again that the results of this study are severely distorted by selection in the range $0.5^m < (B_T - V_T)_0 < 0.7^m$.

However, this test exclusion of stars from the sample of Gontcharov (2012c) hardly affected the results in the range $-0.05^m < (B_T - V_T)_0 < 0.1^m$, but, at the same time, the results of the two studies come considerably closer together when using the same parallaxes and proper motions. Consequently, in this range, i.e., for stars of late B subtypes and early A subtypes, TGAS gives parallaxes and proper motions that differ systematically from those in Hipparcos. This is particularly clearly seen for the velocity component U_\odot in Fig. 4a. Thus, according to TGAS, these B- and A-type stars, which are observed at Galactic longitudes of about 90° and 270° and, hence, belong to the Local spiral arm, move toward the Galactic anticenter, on average, 3 km s^{-1} faster and show a smaller scatter of velocities than that from the Hipparcos data. The next, more complete Gaia data releases can answer the question of whether this is the result of an increase in the Gaia accuracy compared to Hipparcos or, on the contrary, the result of zonal systematic errors in TGAS.

The last systematic deviation from the main set of results is that in Figs. 3b and 4b the results of Dehnen and Binney (1998) (black triangles) at $0.08^m < (B_T - V_T)_0 < 0.38^m$ show very small V_\odot . This may stem from the fact that Dehnen and Binney (1998) did not use V_r .

Returning to the list of possible causes of the discrepancies between the results of the studies given in the Introduction, we will note the following:

1. Dehnen and Binney (1998) used the data from the first Hipparcos version, while Aumer and Binney (2009) used those from the new one. Otherwise these studies are very similar. In Fig. 2a we see a coincidence between the results of these studies at $(B_T - V_T)_0 < 0.4^m$ and systematically smaller σ_U in Aumer and Binney (2009). Apparently, the transition from the first Hipparcos version to the new one manifested itself in this way.
2. Aumer and Binney (2009) and Aghajani and Lindegren (2013) tested the influence of the radial velocities on their results. In the range $0.25^m < (B_T - V_T)_0 < 0.5^m$ the dispersions derived with and without V_r almost coincided. However, in the range $0.5^m < (B_T - V_T)_0 < 0.7^m$ invoking V_r in both studies systematically increased the dispersions by $1\text{--}4 \text{ km s}^{-1}$, while U_\odot , V_\odot and W_\odot did not change.
3. The various effects of selection have been shown previously. We will only add that in combating them, Dehnen and Binney (1998) proposed to impose strong magnitude constraints on the samples. Francis and Anderson (2009) argued against the necessity of this by showing that the GCS, PCRV, and CRVAD-2 catalogues of radial velocities produce

selection that causes no significant biases of the kinematic characteristics. At the same time, Gontcharov (2009a) showed that due to the strong correlation of the apparent magnitude, the absolute magnitude, the absolute value of the proper motion, the parallax, and the errors of these quantities for MS stars, any constraint or selection by any of these characteristics, in general, causes biases of the kinematic characteristics being determined. Consequently, they are present in all of the results under consideration, including the results of Dehnen and Binney (1998). Tests like those performed in this study are needed to reveal these biases.

4. For the results of Mignard (2000) and Aghajani and Lindegre (2013) $(B_T - V_T)_0$ were calculated from the spectral type and the $(b - y)$ color, respectively. Nevertheless, it can be seen from Figs. 2, 4, and 5 that their results agree well with the remaining ones. We will add that, in general, the uncertainties of the calibrations (for example, $(B_T - V_T)_0$ from $(b - y)$) are currently smaller than the uncertainties of the reddening estimates. Therefore, greater attention should be given to the latter.

DISCUSSION

The studies from Table 1 that showed no significant methodological flaws (Dehnen and Binney 1998; Mignard 2000; Aumer and Binney 2009; Gontcharov 2012; Aghajani and Lindegren 2013) at $-0.1^m < (B_T - V_T)_0 < 0.5^m$ in Figs. 2 and 4 demonstrate agreement between themselves and with the results of this study within $\pm 2 \text{ km s}^{-1}$. Their agreement within ± 0.05 can be seen in Fig. 5. Both these quantities lie within the formal accuracy estimates for these studies. At the same time, the variations of σ_U , σ_V , σ_W , U_\odot , V_\odot , W_\odot , σ_V/σ_U and σ_W/σ_U in the same figures exceed noticeably $\pm 2 \text{ km s}^{-1}$ and ± 0.05 . For example, a well-known growth of the dispersion with dereddened color and age can be seen in Fig. 2. Given the dependences (1) and (2), it can be described by the dependences derived by the least-squares method from all reliable data (in km s^{-1}):

$$\sigma_U = 16.0e^{1.29(B_T - V_T)_0}, \sigma_V = 10.9e^{1.11(B_T - V_T)_0}, \sigma_W = 6.8e^{1.46(B_T - V_T)_0}. \quad (3)$$

They correspond to

$$\beta_U = 0.33, \beta_V = 0.285, \beta_W = 0.37. \quad (4)$$

The results of all these best studies fit into the range ± 0.05 relative to these values. However, these values of β refer only to comparatively young stars in the ranges of colors $-0.1^m < (B_T - V_T)_0 < 0.5^m$ and ages from 0.23 to 2.4 Gyr. Therefore, we can draw only cautious conclusions, especially pending more accurate Gaia data. However, it can be argued that with a high probability

$$\beta_V < \beta_U < \beta_W, \quad (5)$$

with β_U and β_W being close to $1/3$ and β_V being between $1/3$ and $1/4$. All three exponents are quite far from the popular estimates of 0.4 – 0.5 in previous studies. A modern overview of β and the corresponding causes of the increase in velocity dispersion with age was given by Aumer et al. (2016). The influence of giant molecular clouds, the spiral pattern, the bar, satellite galaxies, a nonuniform distribution of dark matter, and, in general, any source of gravity causing a deviation of the Galactic gravitational field in the solar neighborhood from the axisymmetric one are among the causes. Yet another cause is a decrease in the initial velocity dispersion of stars during their birth as the Galaxy evolves due to the decrease in the total gas mass in the

disk. Aumer et al. (2016) simulated the influence of many of these causes on β and concluded that the spiral pattern, the bar, and giant molecular clouds play a key role. When comparing the results of Aumer et al. (2016) with β from this study, the discrepancy in β_W is particularly pronounced. Only one of the models of Aumer et al. (2016), Y1s2, gives $\beta_W = 0.41$ comparable to that obtained in this study. The remaining models give much larger values. Consequently, the results of this study argue for the parameters of the Galaxy that provide a low value of β_W . Aumer et al. (2016) pointed out these parameters: a more constant star formation rate causing a slow decrease in the mass of giant molecular clouds as the Galaxy evolves; giant molecular clouds play an important, but not exceptional role in the growth of the velocity dispersion, including σ_W ; a comparatively large mass (including the dark halo) lies far from the Galactic plane. They also proposed a scenario providing a minimum β_W when the condition (5) is met precisely for comparatively young stars, as in this study: the spiral pattern, at a secondary role of giant molecular clouds, causes an increase in σ_U and σ_V only until some moment, and giant molecular clouds then continue to increase σ_W , turning the orbits of stars with a large eccentricity and a small inclination to the Galactic plane into orbits with a small eccentricity and a large inclination. Aumer et al. (2016) pointed out that the ratio σ_W/σ_U is a measure of the influence of giant molecular clouds or the spiral pattern that increase the stellar velocity dispersions, respectively, in all directions or only along the Galactic plane. The gradual growth in σ_W/σ_U with stellar age found in this study corresponds to the assumption made by Aumer et al. (2016) about an increase in the relative importance of the spiral pattern compared to the importance of clouds, which are expended to a considerable extent on star formation.

U_\odot , V_\odot and W_\odot variations with an amplitude of 7, 9, and 2.7 km s⁻¹, respectively, can be seen in Figs. 4a–4c. The latter value is small enough to adopt the mean and the range of variations around it in km s⁻¹ for the entire range $-0.1^m < (B_T - V_T)_0 < 0.5^m$:

$$\overline{W_\odot} = 7.15 \pm 1.35. \quad (6)$$

In the same range the U_\odot and V_\odot variations in km s⁻¹ can be fitted by the dependences derived from all reliable studies:

$$U_\odot = 782(B_T - V_T)_0^4 - 698(B_T - V_T)_0^3 + 225.6(B_T - V_T)_0^2 - 23.5(B_T - V_T)_0 + 10.38 \quad (7)$$

$$V_\odot = 1228(B_T - V_T)_0^4 - 1214(B_T - V_T)_0^3 + 319(B_T - V_T)_0^2 - 8.8(B_T - V_T)_0 + 8.34. \quad (8)$$

These relations do not reflect the high-frequency variations that, for example, are visible in the results of Dehnen and Binney (1998) and this study: the local maximum of U_\odot and V_\odot at $(B_T - V_T)_0 \approx 0.23^m$, another local maximum of U_\odot at $(B_T - V_T)_0 \approx 0.35^m$, and two local minima of U_\odot at $(B_T - V_T)_0 \approx 0.29^m$ and 0.41^m . These studies are completely independent, did not use any common data, and Dehnen and Binney (1998) did not use V_r at all. Therefore, these extrema can be real and need a further study.

The dependence for V_\odot is a manifestation of the well-known asymmetric drift, i.e., the dependence of the rotation velocity of stars around the Galactic center on their age (Perryman 2009, p. 305). It can be seen from Fig. 4 that at $(B_T - V_T)_0 > 0.04^m$, i.e., at an age older than 0.4 Gyr, V_\odot increases with $(B_T - V_T)_0$, though not monotonically. The theoretical linear dependence of V_\odot on the age (Francis and Anderson 2009) is not confirmed: in addition to it, there are high-frequency variations. It is also obvious that stars of approximately the same, accurately determined age should be used for any estimates of the peculiar solar motion relative to the group of stars (for a discussion, see Gontcharov 2012c).

In Fig. 5 the σ_V/σ_U and σ_W/σ_U variations reach ± 0.1 and ± 0.07 , respectively. σ_V/σ_U and σ_W/σ_U change their behavior in unison: at $(B_T - V_T)_0 < 0.25^m$, i.e., at an age younger than 0.9 Gyr, σ_V/σ_U decreases with $(B_T - V_T)_0$ and $\sigma_W/\sigma_U = 0.42 \pm 0.05$ is constant, while at $0.25^m < (B_T - V_T)_0 < 0.5^m$ $\sigma_V/\sigma_U = 0.63 \pm 0.05$ is constant and σ_W/σ_U increases with $(B_T - V_T)_0$ to $\sigma_W/\sigma_U \approx 0.55$. For comparison, Famaey et al. (2005) found stabilization for branch giants with an age older than 3 Gyr at $\sigma_V/\sigma_U = 0.65$ and $\sigma_W/\sigma_U = 0.50$, i.e., close to our values. However, their simulations gave 0.79 and 0.55, where the former differs greatly from the empirical values.

It can be seen from Fig. 2 that, on the whole, σ_U and σ_V adopted in the BMG (stepwise curve) at $(B_T - V_T)_0 > 0^m$ describe satisfactorily the growth of these dispersions with dereddened color and age, while for σ_W they are clearly underestimated. At $(B_T - V_T)_0 < 0^m$ the BMG values were clearly overestimated. In the BMG the thin-disk stars were separated by age into seven populations with discrete values of their kinematic characteristics. This gives the stepwise pattern of the dependences for the BMG in Figs. 1, 2, and 5. A comparison of these dependences with the remaining results shows that the kinematic characteristics of the stars under consideration change gradually rather than abruptly, as in the BMG.

CONCLUSIONS

In recent years, the original data traditionally used to study the kinematics of stars near the Sun have been updated substantially. The Gaia DR1 TGAS catalogue gave the most accurate parallaxes and proper motions, the PARSEC, MIST, YAPSI, and BaSTI databases gave improved theoretical isochrones, a number of studies with reddening and interstellar extinction estimates near the Sun have appeared. These data were tested in our study when calculating the dependences of kinematic characteristics on the dereddened color and the age correlating with it. The age was taken from the Geneva-Copenhagen survey in agreement with the estimates of the theoretical TRILEGAL database. The radial velocities were taken from the PCRV, which covers the entire sky and is most free from the systematic errors. The parallax and radial velocity errors were shown to introduce the main uncertainty into the results.

Based on the criterion $(B_T - V_T)_0 < 0.7^m$, for our study we chose a region of the HR diagram that is kinematically interesting and sensitive to the data accuracy: B-F types of the MS. We selected 9543 thin-disk stars with accurate Tycho-2 photometry and parallaxes $\sigma(\varpi)/\varpi < 0.1$. This provided a median relative accuracy of 1.7 km s^{-1} for the velocity components U , V , and W , the highest one among all studies of kinematic characteristics.

We considered the variations of σ_U , σ_V , σ_W , U_\odot , V_\odot , W_\odot , σ_V/σ_U and σ_W/σ_U with $(B_T - V_T)_0$ in comparison with the key results of other authors obtained after the appearance of the Hipparcos catalogue. Various tests showed a significant effect of selection on the kinematic characteristics, especially outside the range $-0.1^m < (B_T - V_T)_0 < 0.5^m$. For example, the excessively stringent and color- and age-independent criteria for the selection of thin-disk stars in the studies of Gómez et al. (1997) and Francis and Anderson (2009) explain the deviation of their results from the remaining ones. The kinematic characteristics calculated from the TGAS data outside the range $-0.1^m < (B_T - V_T)_0 < 0.5^m$ are also significantly biased due to selection in TGAS. However, in the range $-0.1^m < (B_T - V_T)_0 < 0.5^m$ the results obtained only from the proper motions or radial velocities are close.

The positions of the stars under consideration on the HR diagram with PARSEC, MIST, YaPSI, and BaSTI isochrones when using different reddening and extinction estimates showed the following: (1) the isochrones are in agreement with one another and (2) the reddening and extinction estimates are erroneous in some kinematic studies. The estimates based on the 3D reddening map from Gontcharov (2017a) in combination with the 3D extinction-to-reddening map from Gontcharov (2012a) were recognized to be the most reliable ones. The colors of the stars used in other studies were corrected for an inaccurate reddening correction.

As a result, the dependences of the kinematic characteristics on $(B_T - V_T)_0$ obtained by various authors approached significantly one another and the results of our study. The scatter of σ_U , σ_V , σ_W , U_\odot , V_\odot and W_\odot in reliable studies in the range $-0.1^m < (B_T - V_T)_0 < 0.5^m$ fits into a $\pm 2 \text{ km s}^{-1}$ corridor, while the scatter of σ_V/σ_U and σ_W/σ_U fits into ± 0.05 . This corresponds to the upper bound of the declared accuracy of the studies under consideration. This allowed the variations of the kinematic quantities as a function of $(B_T - V_T)_0$ and age in relations (3)–(8) to be reliably determined. These variations make the determination of the solar motion relative to the stars without specifying their age meaningless.

ACKNOWLEDGMENTS

I am grateful to the referees for their useful remarks. In this study I used resources from the Strasbourg Astronomical Data Center (<http://cdsweb.ustrasbg.fr>) and Hipparcos/Tycho results. In this study I used data from the Gaia mission of the European Space Agency (<https://www.cosmos.esa.int/gaia>) processed by the Gaia Data Processing and Analysis Consortium (DPAC, <https://www.cosmos.esa.int/web/gaia/dpac/consortium>).

References

1. A. Abergel, P. A. R. Ade, N. Aghanim, M. I. R. Alves, G. Aniano, C. Armitage-Caplan, M. Arnaud, et al. (Planck Collab.), *Astron. Astrophys.* **571**, A11 (2014).
2. F. Arenou, M. Grenon, and A. Gómez, *Astron. Astrophys.* **258**, 104 (1992).
3. T.-L. Astraatmadja and C.A.L. Bailer-Jones, *Astrophys. J.* **833**, 119 (2016).
4. M. Aumer and J.J. Binney, *Mon. Not. R. Astron. Soc.* **397**, 1286 (2009).
5. M.Aumer, J. Binney, and R. Schönrich, *Mon. Not. R. Astron. Soc.* **462**, 1697 (2016).
6. J. Bovy, *Mon. Not. R. Astron. Soc.* **468**, 63 (2017).
7. A. Bressan, P. Marigo, L. Girardi, B. Salasnich, C. Dal Cero, S. Rubele, and A. Nanni, *Mon. Not. R. Astron. Soc.* **427**, 127 (2012), <http://stev.oapd.inaf.it/cmd>.
8. A.G.A. Brown, A. Vallenari, T. Prusti, J.H.J. de Bruijne, F. Mignard, R. Drimmel, C. Babusaix, C. A.L. Bailer-Jones, et al. (Gaia Collab.), *Astron. Astrophys.* **595**, A2 (2016).
9. J.A. Cardelli, G.C. Clayton, and J.S. Mathis, *Astrophys. J.* **345**, 245 (1989).

10. L. Casagrande, R. Schönrich, M. Asplund, S. Cassisi, I. Ramírez, J. Meléndez, T. Bensby, and S. Feltzing, *Astron. Astrophys.* **530**, A138 (2011).
11. J. Choi, A. Dotter, C. Conroy, M. Cantiello, B. Paxton, B.D. Johnson, *Astrophys. J.* **823**, 102 (2016).
12. M.A. Czekaj, A.C. Robin, F. Figueras, X. Luri, and M. Haywood, *Astron. Astrophys.* **564**, A102 (2014).
13. W. Dehnen and J. Binney, *Mon. Not. R. Astron. Soc.* **294**, 429 (1998).
14. A. Dotter, *Astrophys. J. Supp. Ser.* **222**, 8 (2016), <http://waps.cfa.harvard.edu/MIST/>
15. ESA, *Hipparcos and Tycho catalogues* (ESA, 1997).
16. B. Famaey, A. Jorissen, X. Luri, M. Mayor, S. Udry, H. Dejonghe, and C. Turon, *Astron. Astrophys.* **430**, 165 (2005).
17. C. Francis and E. Anderson, *New Astronomy* **14**, 615 (2009).
18. L. Girardi, M.A.T. Groenewegen, E. Hatziminaoglou, L. da Costa, *Astron. Astrophys.* **436**, 895, (2005), <http://stev.oapd.inaf.it/cgi-bin/trilegal>
19. A.E. Gómez, S. Grenier, S. Udry, M. Haywood, L. Meillon, V. Sabas, A. Sellier, and D. Morin, *Proceedings of the ESA Symp. "Hipparcos - Venice 97"*, *ESA SP-402*, Ed. B. Battick, *ESA Publications Division, c/o ESTEC, Noordwijk, The Netherlands*, 621 (1997).
20. G.A. Gontcharov, *Astron. Lett.* **32**, 759 (2006).
21. G.A. Gontcharov, *Astron. Lett.* **33**, 390 (2007).
22. G.A. Gontcharov, *Astron. Lett.* **35**, 638 (2009a).
23. G.A. Gontcharov, *Astron. Lett.* **35**, 780 (2009b).
24. G.A. Gontcharov, *Astron. Lett.* **37**, 707 (2011).
25. G.A. Gontcharov, *Astron. Lett.* **38**, 12 (2012a).
26. G.A. Gontcharov, *Astron. Lett.* **38**, 87 (2012b).
27. G.A. Gontcharov, *Astron. Lett.* **38**, 771 (2012c).
28. G.A. Gontcharov, *Astron. Lett.* **43**, 472 (2017a).
29. G.A. Gontcharov, *Astron. Lett.* **43**, 545 (2017b).
30. G.A. Gontcharov and A.T. Bajkova, *Astron. Lett.* **39**, 689 (2013).
31. G.A. Gontcharov and A.V. Mosenkov, *Mon. Not. R. Astron. Soc.* **470**, L97 (2017a).
32. G.A. Gontcharov and A.V. Mosenkov, *Mon. Not. R. Astron. Soc.* **472**, 3805 (2017b).
33. G.A. Gontcharov, A.A. Andronova, O.A. Titov, and E.V. Kornilov, *Astron. Astrophys.* **365**, 222 (2001).

34. G.A. Gontcharov, A.T. Bajkova, P.N. Fedorov, and V.S. Akhmetov, *Mon. Not. R. Astron. Soc.* **413**, 1581 (2011).
35. G.M. Green, E.F. Schlafly, D.P. Finkbeiner, H.-W. Rix, N. Martin, W. Burgett, P.W. Draper, et al., *Astrophys. J.* **810**, 25 (2015), <http://argonaut.skymaps.info>
36. M. Haywood, *Mon. Not. R. Astron. Soc.* **371**, 1760 (2006).
37. E. Høg, C. Fabricius, V.V. Makarov, S. Urban, T. Corbin, G. Wycoff, U. Bastian, P. Schwendiek, and A. Wicenecet, *Astron. Astrophys.* **355**, L27 (2000).
38. J. Holmberg, B. Nordström, and J. Andersen, *Astron. Astrophys.* **475**, 519 (2007).
39. J. Holmberg, B. Nordström, and J. Andersen, *Astron. Astrophys.* **501**, 941 (2009).
40. N.V. Kharchenko, R.-D. Scholz, A.E. Piskunov, S. Röser, and E. Schilbach, *Astronomische Nachrichten* **328**, 889 (2007).
41. P. G. Kulikovskii, *Stellar Astronomy* (Nauka, Moscow, 1985) [in Russian].
42. A. Kunder, G. Kordopatis, M. Steinmetz, T. Zwitter, P.J. McMillan, L. Casagrande, H. Enke, J. Wojno, et al., *Astron. J.* **153**, 75 (2017), <http://www.rave-survey.org>
43. F. van Leeuwen, *Astron. Astrophys.* **474**, 653 (2007).
44. A.M. Meisner and D.P. Finkbeiner, *Astrophys. J.* **798**, 88 (2015).
45. D. Michalik, L. Lindegren, and D. Hobbs, *Astron. Astrophys.* **574**, A115 (2015).
46. F. Mignard, *Astron. Astrophys.* **354**, 522 (2000).
47. B. Nordström, M. Mayor, J. Andersen, J. Holmberg, F. Pont, B.R. Jørgensen, E.H. Olsen, S. Udry, et al., *Astron. Astrophys.* **418**, 989 (2004).
48. P. P. Parenago, *A Course in Stellar Astronomy* (GITTL, Moscow, 1954) [in Russian].
49. B. Paxton, L. Bildsten, A. Dotter, F. Herwig, P. Lesaffre, and F. Timmes, *Astrophys. J. Supp. Ser.* **192**, 3 (2011).
50. M. Perryman, *Astronomical Applications of Astrometry* (Cambridge Univ. Press, Cambridge, 2009).
51. A. Pietrinferni, S. Cassisi, M. Salaris, and F. Castelli, *Astrophys. J.* **612**, 168 (2004), <http://basti.oa-teramo.inaf.it>
52. A.C. Robin, C. Reylé, S. Derrière, and S. Picaud, *Astron. Astrophys.* **409**, 523 (2003).
53. D.J. Schlegel, D.P. Finkbeiner, and M. Davis, *Astrophys. J.* **500**, 525 (1998).
54. S. Sharma, J. Bland-Hawthorn, J. Binney, K.C. Freeman, M. Steinmetz, C. Boeche, O. Bienaymé, B.K. Gibson, G.F. Gilmore, et al., *Astrophys. J.* **793**, 51 (2014).
55. M.F. Skrutskie, R.M. Cutri, R. Stiening, M.D. Weinberg, S. Schneider, J.M. Carpenter, C. Beichman, R. Capps, et al., *Astron. J.* **131**, 1163 (2006), <http://www.ipac.caltech.edu/2mass/releases/allsky/index.html>

56. F. Spada, P. Demarque, Y.-C. Kim, T.S. Boyajian, J.M. Brewer, *Astrophys. J.* **838**, 161 (2017), <http://www.astro.yale.edu/yapsi/>
57. H.-J. Tian, C. Liu, J.L. Carlin, Y.-H. Zhao, X.-L. Chen, Y. Wu, G.-W. Li, Y.-H. Hou, and Y. Zhang, *Astrophys. J.* **809**, 145 (2015).